



Tritium-labeled agonists as tools for studying adenosine A_{2B} receptors

Sonja Hinz¹ · Wessam M. Alnouri¹ · Ulrich Pleiss² · Christa E. Müller¹

Received: 8 January 2018 / Accepted: 27 April 2018 / Published online: 11 May 2018
© Springer Science+Business Media B.V., part of Springer Nature 2018

Abstract

A selective agonist radioligand for A_{2B} adenosine receptors (A_{2B}ARs) is currently not available. Such a tool would be useful for labeling the active conformation of the receptors. Therefore, we prepared BAY 60-6583, a potent and functionally selective A_{2B}AR (partial) agonist, in a tritium-labeled form. Despite extensive efforts, however, we have not been able to establish a radioligand binding assay using [³H]BAY 60-6583. This is probably due to its high non-specific binding and its moderate affinity, which had previously been overestimated based on functional data. As an alternative, we evaluated the non-selective A_{2B}AR agonist [³H]NECA for its potential to label A_{2B}ARs. [³H]NECA showed specific, saturable, and reversible binding to membrane preparations of Chinese hamster ovary (CHO) or human embryonic kidney (HEK) cells stably expressing human, rat, or mouse A_{2B}ARs. In competition binding experiments, the AR agonists 2-chloroadenosine (CADO) and NECA displayed significantly higher affinity when tested versus [³H]NECA than versus the A_{2B}-antagonist radioligand [³H]PSB-603 while structurally diverse AR antagonists showed the opposite effects. Although BAY 60-6583 is an A_{2B}AR agonist, it displayed higher affinity versus [³H]PSB-603 than versus [³H]NECA. These results indicate that nucleoside and non-nucleoside agonists are binding to very different conformations of the A_{2B}AR. In conclusion, [³H]NECA is currently the only useful radioligand for determining the affinity of ligands for an active A_{2B}AR conformation.

Keywords Adenosine A_{2B} receptor · Agonist radioligand · [³H]BAY 60-6583 · [³H]NECA · Kinetics · Radioligand binding

Abbreviations

[¹²⁵ I]ABOPX	2-[4-[3-[(4-Amino-3-iodobenzyl)]-2,6-dioxo-1-propyl-7H-purin-8-yl]phenoxy]acetic acid	CGS-21680	(2- <i>p</i> -[2-Carboxyethyl]phenethylamino)-5'- <i>N</i> -ethylcarboxamidoadenosine
ADA	Adenosine desaminase	DPCPX	1,3-Dipropyl-8-cyclopentylxanthine
AR	Adenosine receptor(s)	CHO	Chinese hamster ovary
BAY 60-6583	2-(6-Amino-3,5-dicyano-4-[4-(cyclopropylmethoxy)phenyl]pyridin-2-yl)sulfanylacetamide	Cl-IB-MECA	2-Chloro- <i>N</i> ⁶ -(3-iodobenzyl)-9-[5-(methyl-carbamoyl)-β-D-ribofuranosyl]adenine
BSA	Bovine serum albumin	DMEM	Dulbecco's modified Eagle's medium
CADO	2-Chloroadenosine	DMSO	Dimethyl sulfoxide
CCPA	2-Chloro- <i>N</i> ⁶ -cyclopentyladenosine	FCS	Fetal calf serum
CGS-15943	9-Chloro-2-(2-furyl)[1,2,4]triazolo-[1,5- <i>c</i>]chinazoline-5-amine	G418	Geneticin
		GPCR	G protein-coupled receptor
		hA _{2B}	Human A _{2B}
		HEK293	Human embryonic kidney
		mA _{2B}	Mouse A _{2B}
		MgCl ₂	Magnesium chloride
		MRE2029-F20	<i>N</i> -Benzo[1,3]dioxol-5-yl-2-[5-(2,6-dioxo-1,3-dipropyl-2,3,6,7-tetrahydropurin-8-yl)-1-methyl-1 <i>H</i> -pyrazol-3-yloxy]-acetamide
		MRS-1754	<i>N</i> -(4-Cyanophenyl)-2-[4-(2,3,6,7-tetrahydro-2,6-dioxo-1,3-dipropyl-1 <i>H</i> -purin-8-yl)-phenoxy]acetamide
		MSX-2	3-(3-Hydroxypropyl)-7-methyl-8-(<i>m</i> -methoxystyryl)-1-propargylxanthine

Electronic supplementary material The online version of this article (<https://doi.org/10.1007/s11302-018-9608-5>) contains supplementary material, which is available to authorized users.

✉ Christa E. Müller
christa.mueller@uni-bonn.de

¹ PharmaCenter Bonn, Pharmaceutical Institute, Pharmaceutical Chemistry I, An der Immenburg 4, 53121 Bonn, Germany

² Bayer Pharma AG, Friedrich-Ebert-Straße 217-333, 42117 Wuppertal, Germany

NECA	5'- <i>N</i> -Ethylcarboxamidoadenosine
OSIP-3309391	<i>N</i> -(2-{2-Phenyl-6-[4-(3-phenylpropyl)piperazine-1-carbonyl]-7 <i>H</i> -pyrrolo[2,3- <i>d</i>]pyrimidin-4-ylaminoethyl}acetamide
PSB-1115	4-(2,3,6,7-Tetrahydro-2,6-dioxo-1-propyl-1 <i>H</i> -purin-8-yl)-benzenesulfonic acid
PSB-298	(8-{4-[2-(2-Hydroxyethylamino)-2-oxoethoxy]phenyl}-1-propyl)xanthine
PSB-603	8-(4-(4-(4-Chlorophenyl)piperazine-1-sulfonyl)phenyl)-1-propylxanthine
rA _{2B}	Rat A _{2B}
R-PIA	<i>N</i> ⁶ -(2-Phenylisopropyl)adenosine
ZM 241385	4-(2-[7-Amino-2-(2-furyl)-[1,2,4]-triazolo[2,3- <i>a</i>][1,3,5]-triazin-5-ylamino]ethyl)phenol

Introduction

The G protein-coupled adenosine receptors (ARs) are divided into four subtypes: A₁, A_{2A}, A_{2B}, and A₃. While A₁ and A₃ARs are coupled to G_i proteins mediating an inhibition of adenylyl cyclase, A_{2A} and A_{2B}ARs are coupled to G_s proteins resulting in a stimulation of the enzyme [1]. The A_{2B}ARs can additionally couple to G_q proteins resulting in phospholipase C activation followed by intracellular calcium release [2]. Depending on the structure of agonists and antagonists, different receptor conformations may be induced and stabilized potentially leading to functional selectivity with regard to different signaling pathways, e.g., G protein activation versus β -arrestin recruitment [3]. GPCRs can also form homo- or heteromeric di- or oligomers [4] which may display an altered pharmacology [5, 6]. ARs are involved in a range of diseases including cardiovascular, nervous system, pulmonary, and kidney disorders, and adenosine mediates various effects including anti-inflammatory and immune-suppressive activity [7]. Therefore, ARs represent therapeutic drug targets, and the development of selective agonists and antagonists for medical applications has been of great interest. The A_{2A} and A_{2B}AR subtypes have recently become major targets in immuno-oncological drug development [8]. The well-investigated A_{2A}AR subtype is typically activated by relatively low nanomolar concentrations of adenosine, whereas the A_{2B}AR subtype requires higher micromolar adenosine concentrations for activation. Only few selective A_{2B}AR agonists have been described, the most prominent one being the non-nucleosidic partial agonist 2-[6-amino-3,5-dicyano-4-[4-(cyclopropylmethoxy)phenyl]pyridin-2-ylsulfanyl]acetamide (BAY 60-6583) [9, 10]. Only very few other potent A_{2B}AR agonists, all derived from the nucleoside adenosine, have been reported, mainly by the group of Baraldi's [11–13], but their degree of selectivity is unclear since A_{2B}AR data obtained in cAMP accumulation assays were compared to A₁, A_{2A}, and

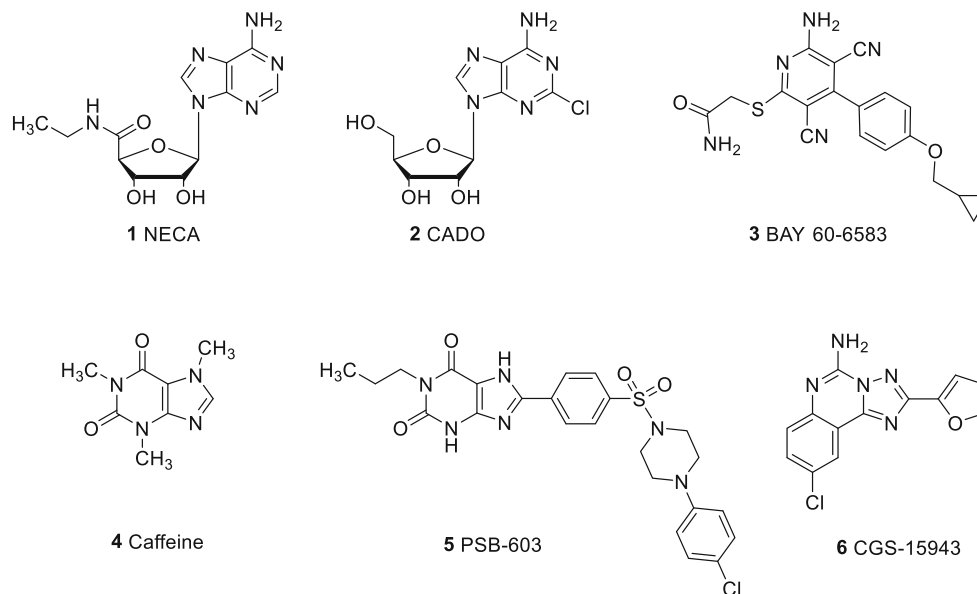
A₃AR radioligand binding data. However, functional assays are highly dependent on receptor expression levels and receptor reserve [14]. In contrast to the situation with agonists, many potent and selective A_{2B}AR antagonists have been developed [13, 15–21] and evaluated in preclinical and initial clinical trials [22]. PSB-603 is one of the most potent and selective A_{2B} antagonists, which is frequently used as a tool compound to study A_{2B}ARs [23–26]. In Fig. 1, a selection of important non-selective and selective A_{2B}AR agonists and antagonists is depicted including NECA, CADO, BAY 60-6583, caffeine, PSB-603, and CGS-15943.

Radioligand receptor binding is a powerful method for the screening of new potential ligands, and the obtained data provide an ideal basis for structure-activity relationship analyses. Agonist radioligands label an active receptor conformation which displays high affinity for agonists while neutral antagonist radioligands bind to active and inactive receptor conformations with similar affinity. Inverse agonist radioligands label an inactive receptor conformation, for which agonists typically display low affinity [27]. For competition binding assays, agonist or antagonist radioligands can be employed, both of which will provide different information about a test compound. While agonists typically show higher affinity when they are tested against agonist radioligands (which label the so-called high-affinity binding site of an active receptor conformation), they usually display lower affinity for an antagonist/inverse agonist radioligand-labeled, inactive receptor conformation. In some cases, biphasic curves are observed in competition binding assays of agonists versus antagonist radioligands, e.g., for the human A₁AR [28]. However, at A_{2A} and A_{2B}ARs, no biphasic curves have been observed and only inactive, low affinity conformations appeared to be labeled by antagonist radioligands [17, 29]. Consequently, A_{2A}AR agonists were found to display lower affinity versus antagonist radioligands than versus agonist radioligands. Thus, agonist radioligands are important tools to study the affinity of agonists at A_{2A}ARs for their high-affinity binding site in the active receptor conformation. Radioligand binding studies have also been crucial for recent X-ray crystallography [30–32] and NMR studies [33] to prove the correct folding of the receptor proteins after isolation and purification.

Several crystal structures of the human A_{2A}AR in complex with agonists [34–36] and antagonists [37–41] have been published, but the X-ray structure of the A_{2B}AR has not been resolved so far. Recently, crystal structures of the A₁AR have been obtained, which provided insights into selectivity among A₁ and A_{2A}AR subtypes [30, 41].

For the A_{2B}AR, potent and selective antagonist radioligands have been developed [15–18]; however, no selective A_{2B}AR agonist radioligand has been described so far. The non-selective AR agonist [³H]NECA has been reported to

Fig. 1 Structures of the the non-selective AR agonist NECA (1), the non-selective AR agonist CADO (2), the selective (partial) A_{2B} AR agonist BAY 60-6583 (3), the non-selective AR antagonist caffeine (4), the selective A_{2B} AR antagonist PSB-603 (5), and the non-selective AR antagonist CGS-15943 (6)



label A_{2B} ARs [42–45]. But a systematic characterization of [3 H]NECA as a radioligand for A_{2B} ARs has not been performed, and the radioligand has not been employed for the determination of affinities of series of ligands. The goal of the present study was to establish an agonist radioligand binding assay at human, rat, and mouse A_{2B} ARs. To this end, our initial strategy was the preparation and utilization of tritium-labeled BAY 60-6583. However, major difficulties in establishing an A_{2B} AR binding assay with [3 H]BAY 60-6583 prompted us to investigate [3 H]NECA as an A_{2B} AR radioligand instead. The radioligand was subsequently used for characterizing the affinities of ligands, in particular agonists, for the high-affinity conformation labeled by the adenosine derivative.

Materials and methods

Materials and (bio)chemicals

[3 H]NECA (15.9 Ci/mmol) was supplied by Perkin Elmer Life and Analytical Science (Rodgau-Jügesheim, Germany). All other chemical reagents were purchased from Sigma-Aldrich (Taufkirchen, Germany), Tocris Biosciences (Bristol, UK), or Roth (Karlsruhe, Germany), unless otherwise stated. BAY 60-6583 was synthesized or purchased from Tocris Biosciences (Bristol, UK). All cell culture media and penicillin-streptomycin solutions were obtained from Invitrogen (Darmstadt, Germany). Fetal calf serum (FCS) and G418 were purchased from Sigma-Aldrich (Taufkirchen, Germany). Cell culture materials (flasks and dishes) were obtained from Labomedic (Bonn, Germany) and Sarstedt (Nümbrecht, Germany), respectively.

Retroviral transfection of GP⁺ env AM12 cells and infection of CHO-K1 cells

CHO cells stably expressing human, rat, or mouse A_{2B} ARs were generated using a retroviral expression system as previously described [46].

Cell culture

CHO cells stably transfected with the human, rat, or mouse A_{2B} AR were maintained in DMEM-F12 medium with 10% FCS, 100 U/ml penicillin, 100 μ g/ml streptomycin, and 0.8 mg/ml G418 at 37 °C and 5% CO₂.

Membrane preparations

Membranes of CHO cells stably expressing human, rat, or mouse A_{2B} ARs were prepared as previously described [16, 46]. Membranes from HEK-h A_{2B} cells which were used for some of the competition binding studies were purchased from Perkin Elmer (Rodgau-Jügesheim, Germany).

Radioligand receptor binding studies

Preparation of [3 H]BAY 60-6583

The radiosynthesis was performed starting from an iodine-substituted precursor in a single step by iodine-tritium exchange catalyzed by palladium black in tetrahydrofuran in the presence of triethylamine as a base. The product was purified and analyzed by RP-HPLC using the following conditions: column: Phenomenex AQUA C18, 5 μ m, mobile phase: acetonitrile:water (1:1), flow rate of 1 and 5 ml/min, respectively. The analytical HPLC chromatogram with radio

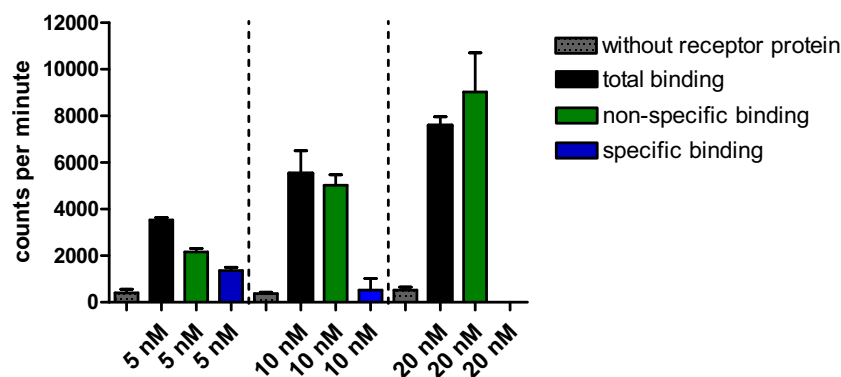


Fig. 2 Binding assays with different concentrations of [3 H]BAY 60-6583. Non-specific binding was determined in the presence of 10 μ M DPCPX. Assay conditions were as follows: a final volume of 500 μ l contained 2.5% DMSO, 50 mM Tris-buffer with 3 mM $MgCl_2$, pH 7.4, as incubation buffer, 5, 10, or 20 nM of [3 H]BAY 60-6583, 80 μ g of

$A_{2B}AR$ membrane preparation per vial, incubation for 140 min at rt, filtration through GF/C filters, and washing with 50 mM ice-cold Tris buffer, pH 7.4. The use of 5 nM of [3 H]BAY 60-6583 gave the best results with 30–40% of specific binding. Data points are means \pm SEM of three (5 nM) or two independent experiments performed in single values

detection and UV detection (254 nm) showed high purity of the product [3 H]BAY 60-6583, which was obtained with a specific radioactivity of 22.7 Ci/mmol (2008.9 MBq/mg) in high radiochemical purity of > 99% (see Supplemental Fig. 1).

Binding experiments with [3 H]BAY 60-6583

Initial binding experiments with [3 H]BAY 60-6583 were performed in a final assay volume of 0.5 ml containing test compound dissolved in DMSO (25 μ l), 275 μ l of assay buffer (50 mM Tris-HCl, pH 7.4), 100 μ l of radioligand solution (1 nM) in assay buffer, and 100 μ l of human $A_{2B}AR$ membrane preparation (30 μ g per vial) suspended in assay buffer containing adenosine deaminase (ADA; 2 U/mg protein, 20 min preincubation at rt). Non-specific binding was determined in the presence of 1 mM NECA, 10 μ M DPCPX, or 10 μ M PSB-1115, respectively. After an incubation time of 30 min at rt, the assay mixture was rapidly filtered through GF/B glass fiber filters using a 24-well Brandel harvester (Brandel, Gaithersburg, MD). Filters were washed three times (3 ml each) with ice-cold 50 mM Tris-HCl buffer, pH 7.4. Then filters were transferred to vials, incubated for 9 h with 2.5 ml of scintillation cocktail (LumaSafe plus, Perkin-Elmer), and counted in a liquid scintillation counter (Tricarb 2700TR) with a counting efficiency of 53%. For additional experiments, a final volume of 0.5 ml, 2.5% DMSO, GF/C filters, higher radioligand concentrations (5, 10, 20 nM), and $MgCl_2$ (3 mM) in the incubation buffer were employed. Additionally, the $A_{2B}AR$ amount was increased to 80 μ g of membrane preparation per vial, and the incubation time was increased to 140 min at rt. Further experiments were conducted at 4 $^{\circ}C$.

Competition binding experiments with [3 H]NECA

Competition binding experiments with [3 H]NECA were performed in a final volume of 1 ml containing 25 μ l of test

compound dissolved in DMSO, 775 μ l of assay buffer (50 mM Tris-HCl, 10 mM $MgCl_2$, pH 7.4), 100 μ l of radioligand solution in assay buffer (final concentration 30 nM), and 100 μ l of human, rat, or mouse $A_{2B}AR$ membrane preparation (200–350 μ g protein or 30 μ g protein (human $A_{2B}AR$ membranes from Perkin Elmer) per vial in assay buffer containing ADA (2 U/mg protein, 20 min incubation at rt). Non-specific binding was determined in the presence of 250 μ M NECA. After an incubation time of 4 h at 4 $^{\circ}C$, the assay mixture was rapidly filtered through GF/C glass fiber filters using a 24-well Brandel harvester (Brandel, Gaithersburg, MD). Filters were washed four times (3 ml each) with ice-cold 50 mM Tris-HCl buffer, pH 7.4. Then filters were transferred to scintillation vials, incubated for 9 h with 2.5 ml of scintillation cocktail (LumaSafe plus, Perkin-Elmer), and counted in a liquid scintillation counter (Tricarb 2700TR) with a counting efficiency of 53%.

Kinetic experiments with [3 H]NECA

Association experiments were performed at 4 $^{\circ}C$ with eight different time points and over a time period of 240 min. Dissociation experiments were initiated after 240 min of preincubation by the addition of 250 μ M NECA. Three separate experiments were performed, each in duplicates. All other conditions were as described above for competition binding experiments.

Saturation binding experiments with [3 H]NECA

Saturation experiments at recombinant human and rat $A_{2B}AR$ s were conducted to determine the K_D values for the radiolabeled agonist NECA at the different species. Different amounts of membrane preparation per vial, which were dependent on the receptor expression (200 μ g for human and 250 μ g for rat), and 7–9 different concentrations of

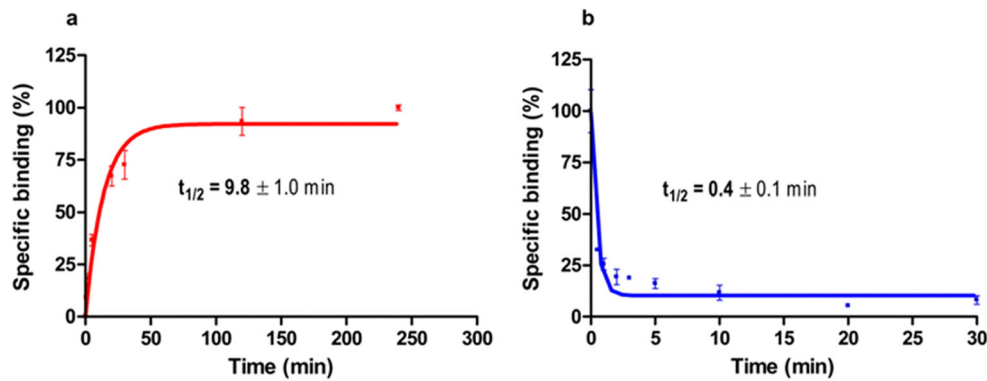


Fig. 3 Binding kinetics of [³H]NECA (30 nM) to membrane preparations of CHO cells recombinantly expressing human A_{2B}ARs. Non-specific binding was determined in the presence of 250 μM NECA. **a** Association experiment. **b** Dissociation experiment. Dissociation was

induced after 240 min of pre-incubation by the addition of 250 μM of unlabeled NECA. Data points are means ± SEM of three separate experiments performed at 4 °C

[³H]NECA in a range of 10–2000 nM were employed. Four (human) or two (rat) separate experiments were performed, each in duplicates. All other assay conditions were as described above for competition binding experiments.

Competition binding experiments with [³H]PSB-603

Competition binding experiments with the antagonist radioligand [³H]PSB-603 at human A_{2B}ARs were performed as previously described [16].

Data analysis

All data were analyzed using Graph Pad Prism, version 4.0 (San Diego, CA, USA). K_D values from homologous competition binding experiments were calculated according to the Cheng and Prusoff equation [47]. In homologous competition binding experiments, radioligand and competitor are the same; therefore, K_D is equal to K_i , and the Cheng and Prusoff equation can be simplified to $K_D = IC_{50} - [\text{radioligand}]$.

Results

Attempts to establish an A_{2B}AR binding assay with [³H]BAY 60-6583

The initial goal of the present study was to establish a radioligand binding assay using the A_{2B}AR agonist [³H]BAY 60-6583. The ³H-labeled form of BAY 60-6583 was obtained from its iodo-substituted precursor by catalytic hydrogenation with tritium gas yielding [³H]BAY 60-6583 with a specific radioactivity of 22.7 Ci/mmol and a high radiochemical purity of >99% (see Supplemental Fig. 1). Initially employed standard radioligand binding assay conditions with 1 nM of [³H]BAY 60-6583, 30 μg of human

A_{2B}AR protein per vial, 30 min incubation time at rt, filtration through GF/B filters, and washing with 50 mM Tris pH 7.4 buffer resulted in high non-specific binding of 80–90% for [³H]BAY 60-6583 (see Supplemental Fig. 2). The addition of 0.1% bovine serum albumin (BSA) to the washing buffer did not reduce non-specific binding (see Supplemental Fig. 3). Further experiments performed at 4 °C with an incubation time of 120 min did not show any increase in specific binding of [³H]BAY 60-6583 (see Supplemental Fig. 4). For subsequent experiments, a final volume of 0.5 ml, 2.5% DMSO, GF/C filters, higher radioligand concentrations (5, 10, 20 nM), and the addition of MgCl₂ (3 mM) to the incubation buffer were tested. Mg²⁺ may shift the A_{2B}AR to an active conformation to which agonists show high affinity as observed for the A_{2A}AR [48]. Under these conditions and with 5 nM of [³H]BAY 60-6583, an increased degree of specific binding of 30–40% could be achieved (Fig. 2). With higher radioligand concentrations, non-specific binding was much higher as could be expected. The moderate specific binding of [³H]BAY 60-6583 was too low to establish a reliable radioligand binding assay, which would require at least 50%, preferably 70% of specific binding. Therefore, different washing buffers were tested. But non-specific binding could not be further reduced, neither by the addition of 5% DMSO nor by adding 5% ethanol to the washing buffer. Many further modifications were tried, including preincubation of the filters in 1% aqueous polyethylenimine solution for 30 min, preincubation of the filters in 0.1% BSA solution, or preincubation of the filters in 50 μM BAY 60-6583 solution, but none of the numerous experiments resulted in increased levels of specific [³H]BAY 60-6583 binding, even in cell membranes with very high expression levels of ca. 10 pmol/mg protein. Because of major difficulties in establishing an A_{2B}AR binding assay with [³H]BAY 60-6583, we subsequently investigated and characterized [³H]NECA as an A_{2B}AR agonist radioligand instead.

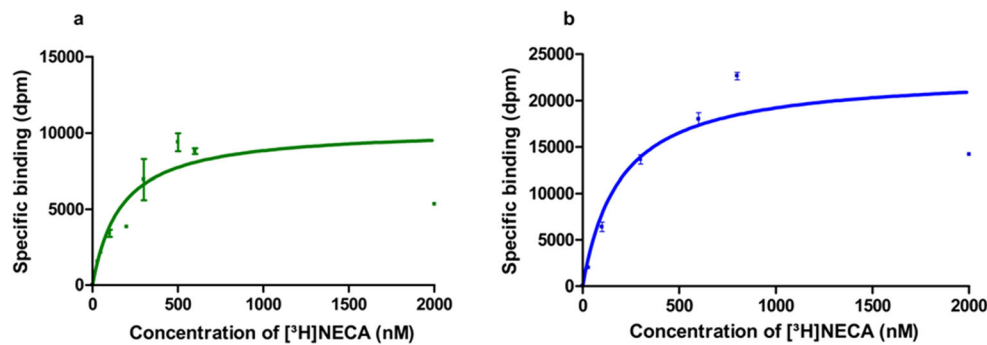


Fig. 4 Saturation binding experiments of [^3H]NECA **a** at human and **b** at rat $\text{A}_{2\text{B}}\text{ARs}$. Non-specific binding was determined in the presence of $250\ \mu\text{M}$ NECA. A K_D value of $441 \pm 169\ \text{nM}$ and a B_{max} value of $2150 \pm 449\ \text{fmol/mg}$ protein were determined for human $\text{A}_{2\text{B}}\text{ARs}$, and

a K_D value of $325 \pm 144\ \text{nM}$ and a B_{max} value of $2680 \pm 472\ \text{fmol/mg}$ protein were determined for rat $\text{A}_{2\text{B}}\text{ARs}$. Data points are means \pm SEM of four (human) or two (rat) independent experiments each performed in duplicates

Radioligand receptor binding studies with [^3H]NECA at recombinant human, mouse, and rat $\text{A}_{2\text{B}}\text{ARs}$

Radioligand binding assays provide quantitative information about receptor expression (B_{max}) and the affinity of ligands (K_i , K_D) at a defined receptor. Three basic protocols, kinetic, saturation, and competition experiments were performed to determine these parameters.

Kinetic experiments

Due to the expected moderate affinity at the human $\text{A}_{2\text{B}}\text{AR}$ and fast dissociation of NECA from the $\text{A}_{2\text{B}}\text{AR}$, kinetic experiments were performed at $4\ ^\circ\text{C}$ using $30\ \text{nM}$ of [^3H]NECA, which gave sufficiently high specific binding (see below). All experiments were best fitted using a single binding site model (Fig. 3a, b). Association (Fig. 3a) reached equilibrium within less than 30 min with a $t_{1/2}$ of $9.7 \pm 1.0\ \text{min}$. Equilibrium binding was stable for at least 240 min. After the addition of a high concentration of unlabeled NECA ($250\ \mu\text{M}$), [^3H]NECA binding was rapidly reversed as shown in Fig. 3b. Because the dissociation ($t_{1/2} = 0.4 \pm 0.1\ \text{min}$) was very fast, much faster than the association, it was not possible to calculate a kinetic K_D value from the k_{on} and k_{off} values.

Next we performed saturation binding experiments to determine K_D and B_{max} values.

Saturation experiments

Saturation binding experiments were carried out using [^3H]NECA on membrane preparations recombinantly expressing $\text{A}_{2\text{B}}\text{ARs}$ of different species, human and rat. [^3H]NECA binding was saturable, and the obtained data were in all cases best fitted to a monophasic curve. For the human $\text{A}_{2\text{B}}\text{AR}$, a K_D value of $441 \pm 169\ \text{nM}$ and a B_{max} value of $2150 \pm 449\ \text{fmol/mg}$ protein were determined (Fig. 4a). The

calculated K_D value was 4-fold lower than the K_i value determined for NECA in competition assays versus the antagonist radioligand [^3H]PSB-603 at human $\text{A}_{2\text{B}}\text{ARs}$ ($1890\ \text{nM}$) [16]. At rat $\text{A}_{2\text{B}}\text{ARs}$, a K_D value of $325 \pm 144\ \text{nM}$ was determined for [^3H]NECA, and a B_{max} value of $2680 \pm 472\ \text{fmol/mg}$ protein was calculated (Fig. 4b). Again, the determined K_D value was about 3-fold lower than the K_i value determined for NECA in competition binding assays versus the antagonist radioligand [^3H]PSB-603 at rat $\text{A}_{2\text{B}}\text{ARs}$ ($1110\ \text{nM}$) [46].

Competition binding experiments

Next, we performed homologous competition binding experiments measuring concentration-dependent inhibition of unlabeled NECA versus [^3H]NECA to determine and compare the K_D and B_{max} values at the different $\text{A}_{2\text{B}}\text{AR}$ species with those obtained in the saturation experiments. At the employed radioligand concentration of $30\ \text{nM}$, specific binding amounted to 50–70% of total binding depending on the harvesting conditions, washing steps, temperature, and membrane preparation. The homologous competition binding experiments resulted in K_D values that were in the same range as those obtained from saturation binding experiments. The calculated K_D and B_{max} values were $663 \pm 87\ \text{nM}$ and $2220 \pm 71\ \text{fmol/mg}$ protein for human $\text{A}_{2\text{B}}\text{ARs}$ (Fig. 5a), $532 \pm 65\ \text{nM}$ and $4400 \pm 1500\ \text{fmol/mg}$ protein for rat $\text{A}_{2\text{B}}\text{ARs}$, and $465 \pm 104\ \text{nM}$ and $1480 \pm 451\ \text{fmol/mg}$ for mouse $\text{A}_{2\text{B}}\text{ARs}$ (Fig. 5b). The competition binding assay conditions were subsequently used for the determination of the affinities of a structurally diverse set of $\text{A}_{2\text{B}}\text{AR}$ ligands, agonists, and antagonists.

For *agonists* determined versus the *agonist radioligand* [^3H]NECA, the following rank order of potency at human $\text{A}_{2\text{B}}\text{ARs}$ was determined: NECA > CADO > BAY 60-6583 (Figs. 5a–d and 6, Supplemental Table 1). For *agonists* determined versus the *antagonist radioligand* [^3H]PSB-603, a

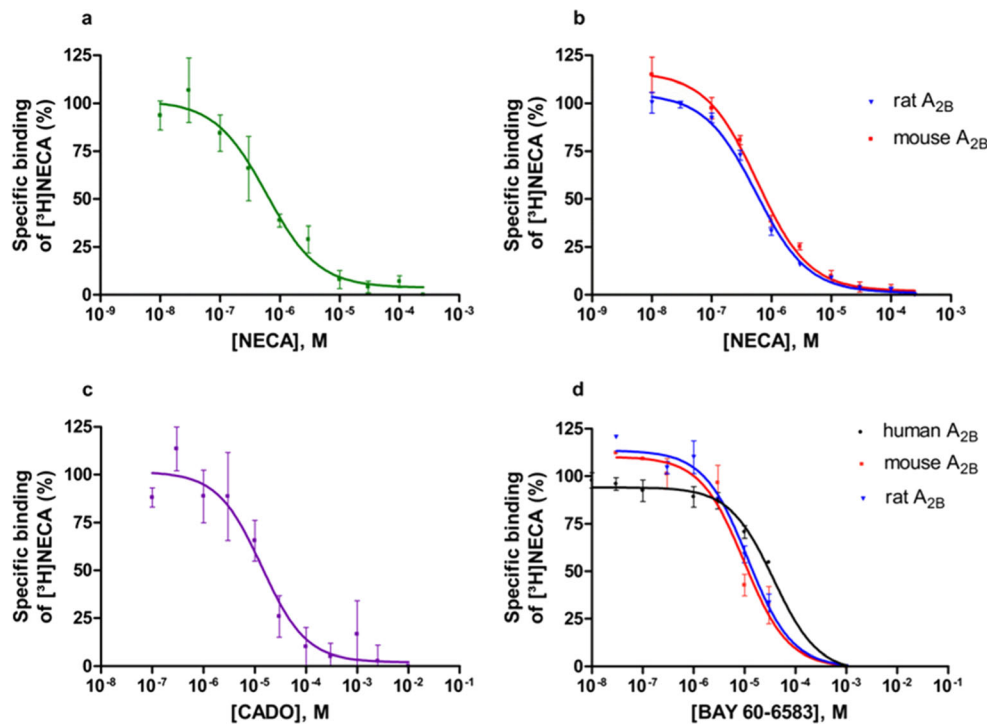


Fig. 5 Homologous competition binding experiments: concentration-dependent inhibition of radioligand binding (30 nM [^3H]NECA) by unlabeled NECA at membrane preparations of CHO cells recombinantly expressing **a** human, **b** rat, or mouse $\text{A}_{2\text{B}}$ ARs. The calculated K_D and B_{max} values were **a** for human $\text{A}_{2\text{B}}$ ARs: 663 ± 87 nM and 2220 ± 71 fmol/mg protein, **b** for rat $\text{A}_{2\text{B}}$ ARs: 532 ± 65 nM and 4400 ± 1500 fmol/mg protein, and for mouse $\text{A}_{2\text{B}}$ ARs: 465 ± 104 nM and 1480 ± 451 fmol/mg protein. Data points are means \pm SEM of three to five independent experiments performed in duplicates. **c** Competition binding of CADO versus 30 nM [^3H]NECA at human $\text{A}_{2\text{B}}$ ARs. A monophasic curve was obtained, and a K_i value of 8570 ± 1110 nM

was determined. Data points are means \pm SEM of four independent experiments each performed in duplicates. **d** Competition binding of BAY 60-6583 versus 30 nM [^3H]NECA at human, mouse, and rat $\text{A}_{2\text{B}}$ ARs. The curves were best fitted by monophasic isotherms. At human $\text{A}_{2\text{B}}$ ARs, a K_i value of $31,400 \pm 7750$ nM, at mouse $\text{A}_{2\text{B}}$ AR, a K_i value of $10,300 \pm 3400$ nM, and at rat $\text{A}_{2\text{B}}$ AR, a K_i value of $10,400 \pm 3430$ nM were determined. In all experiments, non-specific binding was determined in the presence of 250 μM NECA. Data points are means \pm SEM of two (mouse), three (rat), or five (human) independent experiments performed in duplicates (curves were extrapolated because of low solubility of the compound at concentrations > 30 μM)

different rank order of potency at human $\text{A}_{2\text{B}}$ ARs was observed: BAY 60-6583 $>$ NECA $>$ CADO (Fig. 6, Supplemental Table 1).

For 2-chloroadenosine (CADO), a monophasic curve was obtained (Fig. 5c), and the determined K_i value versus [^3H]NECA was about 3-fold lower than that determined versus the antagonist radioligand [^3H]PSB-603 (Fig. 6). Likewise, the K_i value determined for NECA at human $\text{A}_{2\text{B}}$ ARs was significantly (4-fold) lower when determined versus [^3H]NECA as compared to the value obtained versus the antagonist radioligand [^3H]PSB-603 (Fig. 6). In contrast, displacement of [^3H]NECA by BAY 60-6583 at human, mouse, and rat $\text{A}_{2\text{B}}$ ARs showed a lower apparent affinity of BAY 60-6583 in comparison with the K_i value determined versus [^3H]PSB-603 (Figs. 5d and 6, Supplemental Table 1).

As a next step, competition binding experiments for the structurally diverse $\text{A}_{2\text{B}}$ AR antagonists caffeine, PSB-603, and CGS-15943 versus the antagonist radioligand [^3H]PSB-603 and versus the agonist radioligand [^3H]NECA were

performed (Fig. 7, Supplemental Fig. 5a, b, c, Supplemental Table 1), and the following rank order of potency was determined: PSB-603 $>$ CGS-15943 $>$ caffeine. Data from competition binding experiments of the antagonists versus [^3H]NECA were best fitted to a monophasic equation (Supplemental Fig. 5a, b, c). All K_i values determined versus the agonist radioligand [^3H]NECA were significantly higher when compared to the K_i values determined versus the antagonist radioligand [^3H]PSB-603. For caffeine, the determined K_i value versus [^3H]NECA was 3-fold higher than that determined versus the antagonist radioligand [^3H]PSB-603 (Fig. 7). Likewise, the K_i value determined for PSB-603 at human $\text{A}_{2\text{B}}$ ARs was significantly (4-fold) higher when determined versus [^3H]NECA as compared to the value obtained versus the antagonist radioligand [^3H]PSB-603 (Fig. 7). The largest difference was observed for the adenine-like antagonist CGS-15943 (12-fold difference). All three investigated antagonists were not able to fully block [^3H]NECA binding (see Supplemental Fig. 5a, b, c) in contrast to the agonists, which completely displaced [^3H]NECA binding.

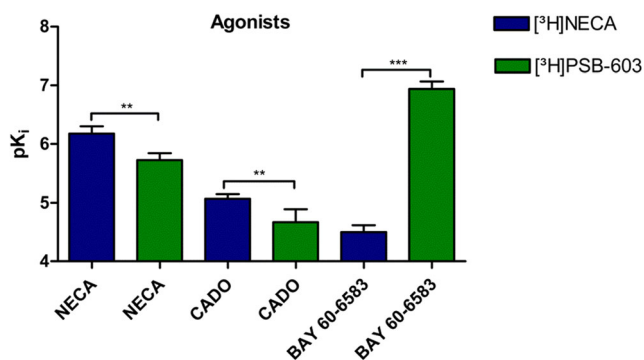


Fig. 6 Affinities of AR agonists determined in competition binding experiments using the agonist radioligand [³H]NECA and the antagonist radioligand [³H]PSB-603 at human A_{2B}ARs. Non-specific binding was determined in the presence of 250 μM NECA ([³H]NECA) or 10 μM DPCPX ([³H]PSB-603). The calculated *K_i* values versus [³H]NECA were 663 ± 87 nM for NECA, 8570 ± 1110 nM for CADO, and 31,400 ± 7750 nM for BAY 60-6583. The calculated *K_i* values versus [³H]PSB-603 were 1890 ± 240 nM for NECA [16], 21,400 ± 5700 nM for CADO [16], and 114 ± 36 nM for BAY 60-6583 [50]. Literature data were from our laboratory performed under the same conditions

Discussion

The initial goal of the present study was to establish a radioligand binding assay with the A_{2B}AR agonist [³H]BAY 60-6583 as a tool for labeling an active A_{2B}AR receptor conformation. BAY 60-6583 had previously been reported to display an EC₅₀ value in the low nanomolar range (3–10 nM) at the human A_{2B}AR as determined in a gene reporter assay [49] combined with high selectivity versus the other AR subtypes (EC₅₀ > 10 μM). However, in radioligand binding assays versus the antagonist radioligand [³H]PSB-603, it had shown a *K_i*

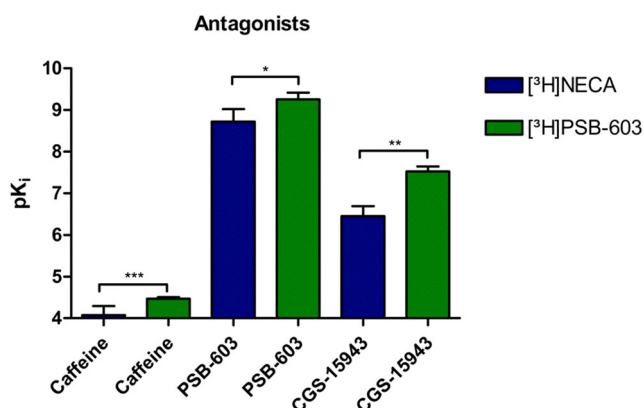


Fig. 7 Competition binding experiments of the antagonists caffeine, PSB-603, and CGS-15943 versus [³H]NECA or [³H]PSB-603 at human A_{2B}ARs. Non-specific binding was determined in the presence of 250 μM NECA ([³H]NECA) or 10 μM DPCPX ([³H]PSB-603). The calculated *K_i* values versus [³H]NECA were 83,700 ± 6000 nM for caffeine, 1.89 ± 0.78 nM for PSB-603, and 357 ± 107 nM for CGS-15943. The calculated *K_i* values versus [³H]PSB-603 were 33,800 ± 1200 nM for caffeine [16], 0.553 ± 0.103 nM for PSB-603 [16], and 30.0 ± 3.9 nM for CGS-15943 [16]. Literature data were from our laboratory performed under the same conditions

value of only 114 nM [50]. Functional assays are highly dependent on receptor expression levels and receptor reserve, and are therefore often not comparable with a compound's receptor affinity. Because of major difficulties in establishing an A_{2B}AR binding assay with [³H]BAY 60-6583 mainly due to its low affinity and high non-specific binding which could not be further reduced with different optimization steps, the compound was not suitable as an agonist radioligand at A_{2B}ARs (see Fig. 2, Supplemental Figs. 2, 3, 4).

Therefore, we characterized the binding of the tritiated non-specific A_{2B}AR agonist NECA at membrane preparations of CHO or HEK cells stably transfected with human, mouse, or rat A_{2B}ARs. Kinetic experiments at human A_{2B}ARs demonstrated that both association and dissociation are monophasic (Fig. 3a, b). Although the experiments were conducted at 4 °C, the association (*t*_{1/2} = 9.7 ± 1.0 min) and in particular the dissociation (*t*_{1/2} = 0.4 ± 0.1 min) were very fast. This relatively fast dissociation is consistent with the moderate affinity of NECA for this receptor subtype. Similarly, fast binding kinetics of [³H]NECA at bovine A_{2B}ARs were reported by Casado et al. [42].

Saturation binding experiments at human and rat A_{2B}ARs were best fitted using a single site binding model (Fig. 4a, b). The determined *K_D* values of 441 ± 169 nM at human A_{2B}ARs and 325 ± 144 nM at rat A_{2B}AR were in the same range as those determined in homologous competition binding experiments (Fig. 5a, b). For mouse A_{2B}ARs, a *K_D* value of 465 ± 104 nM was determined in homologous competition binding experiments (Fig. 5b). The *B_{max}* values determined with [³H]NECA at membrane preparations of recombinant cell lines expressing human, mouse, or rat A_{2B}ARs were around 2000 fmol/mg protein and thus higher than those determined with the antagonist [³H]PSB-603 at human (502 ± 57 fmol/mg protein) and mouse (645 ± 51 fmol/mg protein) A_{2B}ARs [16]. In a native cell system, when no agonist is present, there are generally more receptors in the G protein-uncoupled, inactive conformational state than in the G protein-coupled, active state. It is believed that neutral antagonists bind to all affinity states with similar affinity, whereas inverse agonists preferably bind to an inactive receptor state. Full agonists prefer or even shift the equilibrium to an active receptor conformation, which they stabilize [51]. One reason for the higher *B_{max}* value determined with [³H]NECA is probably the fact that MgCl₂ was included in the agonist assays. Mg²⁺ ions increase the coupling of the A_{2B}ARs to G proteins and therefore promote the active receptor conformation [52]. At A_{2A}ARs, it was found that MgCl₂ increased agonist radioligand binding, e.g., for [³H]NECA and [³H]CGS21680, and reduced non-specific binding [53].

In contrast, PSB-603 is an inverse agonist detecting the inactive receptor state. The affinity of the adenosine derivatives NECA and CADO was approximately 3–4-fold higher when tested versus the agonist radioligand than versus

[³H]PSB-603, which would be expected for agonists. In contrast, the determined A_{2B}AR affinities for structurally diverse antagonists were higher when tested versus the antagonist as compared to agonist radioligand (Fig. 7, Supplemental Table 1).

For the A_{2A}AR, similar differences between agonists and antagonists had previously been observed [52]: *K_i* values of agonists determined versus the antagonist radioligand [³H]MSX-2 were 3–7 times higher than *K_i* values determined versus the agonist radioligand [³H]CGS-21680 [29]. Also, for the A₁AR, it was shown that there is a significant rightward shift in agonist binding curves, most pronounced for rat brain A₁ARs, when using an antagonist radioligand rather than an agonist radioligand (Supplemental Table 2), and this discrepancy may be used to functionally characterize A_{2A}AR ligands for differentiation between agonists and antagonists. For human recombinant A₁ARs, however, this observation could not be confirmed [54]. It appears that the decrease in affinity may be species or cell context-dependent.

Although BAY 60-6583 is a potent A_{2B}AR agonist [9], it showed a large rightward shift in affinity when tested versus the agonist radioligand [³H]NECA as compared to binding studies versus the antagonist/inverse agonist radioligand [³H]PSB-603 (Figs. 5d and 6, Supplemental Table 1). Thus, BAY 60-6583 behaved like the antagonists, not like the agonists. Because it is structurally very different from adenosine derivatives, which are characterized by a nucleoside structure featuring a ribosyl residue (see Fig. 1), the (partial) agonist BAY 60-6583 might stabilize a very different receptor conformation than the full agonist NECA.

Moreover, it was observed that [³H]NECA binding could not be fully displaced by the antagonists, while [³H]PSB-603 binding was fully blocked by the compounds. This may suggest different binding modes of nucleosides (adenosine-derived agonists) on the one hand and antagonists on the other hand (see Supplemental Fig. 5a, b, c). Another more likely explanation would be the presence of a previously described NECA-binding protein designated adenotin [55, 56]. Adenotin, which was later identified as heat shock protein paralog Grp94 [57], was reported to display submicromolar affinity for NECA and to lack affinity for adenosine receptor antagonists [55, 56]. Saturation analysis with soluble and membrane-derived adenotin had shown a *K_D* value for NECA of 220 nM (soluble) and 210 nM (membrane-derived) [56]. In a previous study performed in chromaffin plasma cell membranes, the xanthine antagonist DPCPX had shown complete inhibition of [³H]NECA binding [42], which might be due to the lack of expression of the NECA-binding protein adenotin in the employed cell line. Binding to non-transfected HEK cell membranes showed some specific binding, which was, however, moderate and may be at least partly due to the endogenous expression of A_{2B}ARs [58] (see SI Fig. S6). In order to avoid effects that are due to binding of

[³H]NECA to potentially present adenotin/Grp94, it may be advisable to use an A_{2B}AR antagonist for the determination of non-specific binding.

Conclusions

[³H]BAY 60-6583, a potent and functionally selective A_{2B}AR (partial) agonist, was prepared and examined as a tool for labelling an active A_{2B}AR conformation. However, despite excessive efforts, we have not been able to establish a radioligand binding assay with this compound mainly due to its high non-specific binding. Nevertheless, [³H]BAY 60-6583 may still be useful for studying in vivo distribution and metabolism of the drug. For the labeling of human, rat, and mouse A_{2B}ARs, we subsequently investigated binding of the non-selective agonist [³H]NECA as an alternative. This adenosine-like agonist labeled A_{2B}ARs with an affinity in the higher nanomolar range and showed acceptable non-specific binding due to its high polarity. [³H]NECA is currently the method of choice for radioligand binding studies aimed at labeling the “high-affinity” active conformation of A_{2B}ARs. Nevertheless, the development of more potent and selective A_{2B}AR agonists would be highly desirable. It has to be pointed out that different agonists are most likely binding to and stabilizing different receptor conformations. This was observed in the present study for adenosine derivatives in comparison to the non-nucleoside (partial) agonist BAY 60-6583, an aminopyridine derivative. Moreover, large affinity differences may be measured for compounds dependent on the structure of the radioligand that is used for affinity determination, since each radioligand may label (induce, stabilize) a specific receptor conformation. X-ray structures of the A_{2B}AR (active conformation) in complex with nucleoside and non-nucleoside agonists would be of great value to further elucidate the receptor’s activation mechanisms.

Acknowledgments We thank Dr. Thomas Krahn, Bayer Healthcare (Germany), for providing [³H]BAY 60-6583.

Compliance with ethical standards

Conflict of interest The authors declare that they have no conflict of interest.

Ethical approval This article does not contain any studies with human participants or animals performed by any of the authors.

References

1. Fredholm BB, IJzerman AP, Jacobson KA, Klotz KN, Linden J (2001) International Union of Pharmacology. XXV. Nomenclature

- and classification of adenosine receptors. *Pharmacol Rev* 53:527–552
2. Gao ZG, Inoue A, Jacobson KA (2017) On the G protein-coupling selectivity of the native A_{2B} adenosine receptor. *Biochem Pharmacol* 17:30706–30720
 3. Wisler JW, Xiao K, Thomsen AR, Lefkowitz RJ (2014) Recent developments in biased agonism. *Curr Opin Cell Biol* 27:18–24
 4. Franco R, Martinez-Pinilla E, Lanciego JL, Navarro G (2016) Basic pharmacological and structural evidence for class A G-protein-coupled receptor heteromerization. *Front Pharmacol* 7:76
 5. Hübner H, Schellhorn T, Gienger M, Schaab C, Kaindl J, Leeb L, Clark T, Möller D, Gmeiner P (2016) Structure-guided development of heterodimer-selective GPCR ligands. *Nat Commun* 7:12298
 6. Hinz S, Navarro G, Borroto-Escuela D, Seibt BF, Ammon YC, de Filippo E, Danish A, Lacher SK, Cervinkova B, Rafahi M, Fuxe K, Schiedel AC, Franco R, Müller CE (2018) Adenosine A_{2A} receptor ligand recognition and signaling is blocked by A_{2B} receptors. *Oncotarget* 9:13593–13611
 7. Jacobson KA, Gao ZG (2006) Adenosine receptors as therapeutic targets. *Nat Rev Drug Discov* 5:247–264
 8. Allard D, Turcotte M, Stagg J (2017) Targeting A₂ adenosine receptors in cancer. *Immunol Cell Biol* 95:333–339
 9. Hinz S, Lacher SK, Seibt BF, Müller CE (2014) BAY60-6583 acts as a partial agonist at adenosine A_{2B} receptors. *J Pharmacol Exp Ther* 349:427–436
 10. Gao ZG, Balasubramanian R, Kiselev E, Wei Q, Jacobson KA (2014) Probing biased/partial agonism at the G protein-coupled A_{2B} adenosine receptor. *Biochem Pharmacol* 90:297–306
 11. Baraldi PG, Preti D, Tabrizi MA, Fruttarolo F, Romagnoli R, Carrion MD, Cara LC, Moorman AR, Varani K, Borea PA (2007) Synthesis and biological evaluation of novel 1-deoxy-1-[6-[(hetero)arylcarbonyl]hydrazino]-9H-purin-9-yl]-N-ethyl-beta-D-ribofuranuronamide derivatives as useful templates for the development of A_{2B} adenosine receptor agonists. *J Med Chem* 50:374–380
 12. Baraldi PG, Tabrizi MA, Fruttarolo F, Romagnoli R, Preti D (2009) Recent improvements in the development of A_{2B} adenosine receptor agonists. *Purinergic Signal* 5:3–19
 13. Müller CE, Baqi Y, Hinz S, Namasivayam, V (2018) Medicinal chemistry of A_{2B} adenosine receptors. In: Borea, P.A. and Varani, K. The adenosine receptors, Springer Science, New York, 2018, **in press**
 14. Kenakin T (2009) Quantifying biological activity in chemical terms: a pharmacology primer to describe drug effect. *ACS Chem Biol* 4:249–260
 15. Baraldi PG, Tabrizi MA, Preti D, Bovero A, Fruttarolo F, Romagnoli R, Moorman AR, Gessi S, Merighi S, Varani K, Borea PA (2004) [³H]-MRE 2029-F20, a selective antagonist radioligand for the human A_{2B} adenosine receptors. *Bioorg Med Chem Lett* 14:3607–3610
 16. Borrmann T, Hinz S, Bertarelli DC, Li W, Florin NC, Scheiff AB, Müller CE (2009) 1-alkyl-8-(piperazine-1-sulfonyl)phenylxanthines: development and characterization of adenosine A_{2B} receptor antagonists and a new radioligand with subnanomolar affinity and subtype specificity. *J Med Chem* 52:3994–4006
 17. Ji X, Kim YC, Ahern DG, Linden J, Jacobson KA (2001) [³H]MRS 1754, a selective antagonist radioligand for A_{2B} adenosine receptors. *Biochem Pharmacol* 61:657–663
 18. Stewart M, Steinig AG, Ma C, Song JP, McKibben B, Castelhan AL, MacLennan SJ (2004) [³H]OSIP339391, a selective, novel, and high affinity antagonist radioligand for adenosine A_{2B} receptors. *Biochem Pharmacol* 68:305–312
 19. El Maatougui A, Azuaje J, Gonzalez-Gomez M, Miguez G, Crespo A, Carbajales C, Escalante L, Garcia-Mera X, Gutierrez-de-Teran H, Sotelo E (2016) Discovery of potent and highly selective A_{2B} adenosine receptor antagonist chemotypes. *J Med Chem* 59:1967–1983
 20. Basu S, Barawkar DA, Ramdas V, Waman Y, Patel M, Panmand A, Kumar S, Thorat S, Bonagiri R, Jadhav D, Mukhopadhyay P, Prasad V, Reddy BS, Goswami A, Chaturvedi S, Menon S, Quraishi A, Ghosh I, Dusange S, Paliwal S, Kulkarni A, Karande V, Thakre R, Bedse G, Rouduri S, Gundu J, Palle VP, Chugh A, Mookhtiar KA (2016) A_{2B} adenosine receptor antagonists: design, synthesis and biological evaluation of novel xanthine derivatives. *Eur J Med Chem* 127:986–996
 21. Carbajales C, Azuaje J, Oliveira A, Loza MI, Brea J, Cadavid MI, Masaguer CF, Garcia-Mera X, Gutierrez-de-Teran H, Sotelo E (2017) Enantiospecific recognition at the A_{2B} adenosine receptor by alkyl 2-cyanoimino-4-substituted-6-methyl-1,2,3,4-tetrahydropyrimidine-5-carboxylates. *J Med Chem* 60:3372–3382
 22. Müller CE, Jacobson KA (2011) Recent developments in adenosine receptor ligands and their potential as novel drugs. *Biochim Biophys Acta* 1808:1290–1308
 23. Doyle C, Cristofaro V, Sack BS, Lukianov SN, Schafer M, Chung YG, Sullivan MP, Adam RM (2017) Inosine attenuates spontaneous activity in the rat neurogenic bladder through an A_{2B} pathway. *Sci Rep* 7:44416
 24. Gnad T, Scheibler S, von Kugelgen I, Scheele C, Kilic A, Glode A, Hoffmann LS, Reverte-Salisa L, Horn P, Mutlu S, El-Tayeb A, Kranz M, Deuther-Conrad W, Brust P, Lidell ME, Betz MJ, Enerback S, Schrader J, Yegutkin GG, Müller CE, Pfeifer A (2014) Adenosine activates brown adipose tissue and recruits beige adipocytes via A_{2A} receptors. *Nature* 516:395–399
 25. Kaji W, Tanaka S, Tsukimoto M, Kojima S (2014) Adenosine A_{2B} receptor antagonist PSB-603 suppresses tumor growth and metastasis by inhibiting induction of regulatory T cells. *J Toxicol Sci* 39:191–198
 26. Vecchio EA, Tan CY, Gregory KJ, Christopoulos A, White PJ, May LT (2016) Ligand-independent adenosine A_{2B} receptor constitutive activity as a promoter of prostate cancer cell proliferation. *J Pharmacol Exp Ther* 357:36–44
 27. Hanania NA, Dickey BF, Bond RA (2010) Clinical implications of the intrinsic efficacy of beta-adrenoceptor drugs in asthma: full, partial and inverse agonism. *Curr Opin Pulm Med* 16:1–5
 28. Lane JR, Klaasse E, Lin J, van Bruchem J, Beukers MW, Ijzerman AP (2010) Characterization of [³H]LUF5834: a novel non-ribose high-affinity agonist radioligand for the adenosine A₁ receptor. *Biochem Pharmacol* 80:1180–1189
 29. Müller CE, Maurinsh J, Sauer R (2000) Binding of [³H]MSX-2 (3-(3-hydroxypropyl)-7-methyl-8-(m-methoxystyryl)-1-propargylxanthine) to rat striatal membranes—a new, selective antagonist radioligand for A_{2A} adenosine receptors. *Eur J Pharm Sci* 10:259–265
 30. Glukhova A, Thal DM, Nguyen AT, Vecchio EA, Jorg M, Scammells PJ, May LT, Sexton PM, Christopoulos A (2017) Structure of the adenosine A₁ receptor reveals the basis for subtype selectivity. *Cell* 168:867–877
 31. Liu X, Ahn S, Kahsai AW, Meng KC, Latorraca NR, Pani B, Venkatakrishnan AJ, Masoudi A, Weis WI, Dror RO, Chen X, Lefkowitz RJ, Kobilka BK (2017) Mechanism of intracellular allosteric beta₂AR antagonist revealed by X-ray crystal structure. *Nature* 548:480–484
 32. Wacker D, Wang S, McCorvy JD, Betz RM, Venkatakrishnan AJ, Levit A, Lansu K, Schools ZL, Che T, Nichols DE, Shoichet BK, Dror RO, Roth BL (2017) Crystal structure of an LSD-bound human serotonin receptor. *Cell* 168:377–389
 33. Fredriksson K, Lottmann P, Hinz S, Onila I, Shymanets A, Harteneck C, Müller CE, Griesinger C, Exner TE (2017) Nanodiscs for INPHARMA NMR characterization of GPCRs:

- ligand binding to the human A_{2A} adenosine receptor. *Angew Chem Int Ed Engl* 56:5750–5754
34. Lebon G, Warne T, Edwards PC, Bennett K, Langmead CJ, Leslie AG, Tate CG (2011) Agonist-bound adenosine A_{2A} receptor structures reveal common features of GPCR activation. *Nature* 474:521–525
 35. Xu F, Wu H, Katritch V, Han GW, Jacobson KA, Gao ZG, Cherezov V, Stevens RC (2011) Structure of an agonist-bound human A_{2A} adenosine receptor. *Science* 332:322–327
 36. Lebon G, Edwards PC, Leslie AG, Tate CG (2015) Molecular determinants of CGS-21680 binding to the human adenosine A_{2A} receptor. *Mol Pharmacol* 87:907–915
 37. Dore AS, Robertson N, Errey JC, Ng I, Hollenstein K, Tehan B, Hurrell E, Bennett K, Congreve M, Magnani F, Tate CG, Weir M, Marshall FH (2011) Structure of the adenosine A_{2A} receptor in complex with ZM241385 and the xanthines XAC and caffeine. *Structure* 19(9):1283–1293
 38. Jaakola VP, Griffith MT, Hanson MA, Cherezov V, Chien EY, Lane JR, Ijzerman AP, Stevens RC (2008) The 2.6 angstrom crystal structure of a human A_{2A} adenosine receptor bound to an antagonist. *Science* 322:1211–1217
 39. Liu Y, Burger SK, Ayers PW, Vohringer-Martinez E (2011) Computational study of the binding modes of caffeine to the adenosine A_{2A} receptor. *J Phys Chem B* 115:13880–13890
 40. Sun B, Bachhawat P, Chu ML, Wood M, Ceska T, Sands ZA, Mercier J, Lebon F, Kobilka TS, Kobilka BK (2017) Crystal structure of the adenosine A_{2A} receptor bound to an antagonist reveals a potential allosteric pocket. *Proc Natl Acad Sci U S A* 114:2066–2071
 41. Cheng RKY, Segala E, Robertson N, Deflorian F, Dore AS, Errey JC, Fiez-Vandal C, Marshall FH, Cooke RM (2017) Structures of human A₁ and A_{2A} adenosine receptors with xanthines reveal determinants of selectivity. *Structure* 25:1275–1285
 42. Casado V, Casillas T, Mallol J, Canela EI, Lluis C, Franco R (1992) The adenosine receptors present on the plasma membrane of chromaffin cells are of the A_{2B} subtype. *J Neurochem* 59:425–431
 43. Corset V, Nguyen-Ba-Charvet KT, Forcet C, Moyse E, Chedotal A, Mehlen P (2000) Netrin-1-mediated axon outgrowth and cAMP production requires interaction with adenosine A_{2B} receptor. *Nature* 407:747–750
 44. Herrera C, Casado V, Ciruela F, Schofield P, Mallol J, Lluis C, Franco R (2001) Adenosine A_{2B} receptors behave as an alternative anchoring protein for cell surface adenosine deaminase in lymphocytes and cultured cells. *Mol Pharmacol* 59:127–134
 45. Mirabet M, Mallol J, Lluis C, Franco R (1997) Calcium mobilization in Jurkat cells via A_{2B} adenosine receptors. *Br J Pharmacol* 122:1075–1082
 46. Alnouri MW, Jepards S, Casari A, Schiedel AC, Hinz S, Müller CE (2015) Selectivity is species-dependent: characterization of standard agonists and antagonists at human, rat, and mouse adenosine receptors. *Purinergic Signal* 11:389–407
 47. Cheng Y, Prusoff WH (1973) Relationship between the inhibition constant K_i and the concentration of inhibitor which causes 50 per cent inhibition I₅₀ of an enzymatic reaction. *Biochem Pharmacol* 22:3099–3108
 48. Johansson B, Parkinson FE, Fredholm BB (1992) Effects of mono- and divalent ions on the binding of the adenosine analogue CGS-21680 to adenosine A₂ receptors in rat striatum. *Biochem Pharmacol* 44:2365–2370
 49. Eckle T, Krahn T, Grenz A, Kohler D, Mittelbronn M, Ledent C, Jacobson MA, Osswald H, Thompson LF, Unertl K, Eltzhischig HK (2007) Cardioprotection by ecto-5'-nucleotidase (CD73) and A_{2B} adenosine receptors. *Circulation* 115:1581–1590
 50. Seibt BF, Schiedel AC, Thimm D, Hinz S, Sherbiny FF, Müller CE (2013) The second extracellular loop of GPCRs determines subtype-selectivity and controls efficacy as evidenced by loop exchange study at A₂ adenosine receptors. *Biochem Pharmacol* 85:1317–1329
 51. Bertarelli DC, Diekmann M, Hayallah AM, Rusing D, Iqbal J, Preiss B, Verspohl EJ, Müller CE (2006) Characterization of human and rodent native and recombinant adenosine A_{2B} receptors by radioligand binding studies. *Purinergic Signal* 2:559–571
 52. Dionisotti S, Ongini E, Zocchi C, Küll B, Arslan G, Fredholm BB (1997) Characterization of human A_{2A} adenosine receptors with the antagonist radioligand [³H]-SCH 58261. *Br J Pharmacol* 121:353–360
 53. Bruns RF, Lu GH, Pugsley TA (1986) Characterization of the A₂ adenosine receptor labeled by [³H]NECA in rat striatal membranes. *Mol Pharmacol* 29:331–346
 54. Klotz KN, Lohse MJ, Schwabe U, Cristalli G, Vittori S, Grifantini M (1989) 2-Chloro-N⁶-[³H]cyclopentyladenosine ([³H]CCPA)-a high affinity agonist radioligand for A₁ adenosine receptors. *Naunyn Schmiedeberg's Arch Pharmacol* 340:679–683
 55. Lorenzen A, Nitsch-Kirsch M, Vogt H, Schwabe U (1993) Characterization of membrane-bound and solubilized high-affinity binding sites for 5'-N-ethylcarboxamido[³H]adenosine from bovine cerebral cortex. *J Neurochem* 60:745–751
 56. Hutchison KA, Nevins B, Perini F, Fox IH (1990) Soluble and membrane-associated human low-affinity adenosine binding protein (adenotin): properties and homology with mammalian and avian stress proteins. *Biochemistry* 29:5138–5144
 57. Gewirth DT (2016) Paralog specific Hsp90 inhibitors—a brief history and a bright future. *Curr Top Med Chem* 16:2779–2791
 58. Cooper J, Hill SJ, Alexander SP (1997) An endogenous A_{2B} adenosine receptor coupled to cyclic AMP generation in human embryonic kidney (HEK293) cells. *Br J Pharmacol* 122:546–550